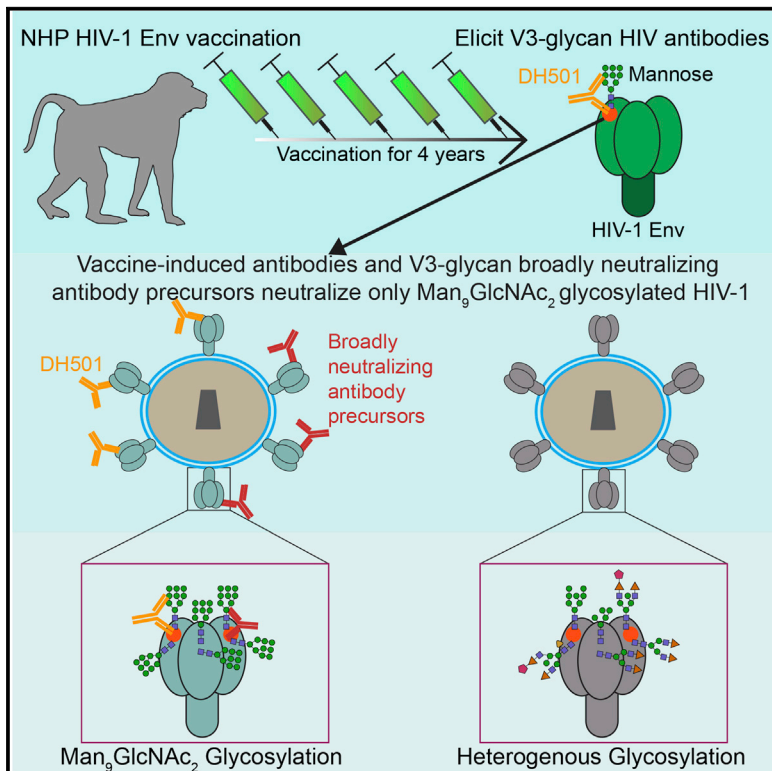# Vaccine Elicitation of High Mannose-Dependent Neutralizing Antibodies against the V3-Glycan Broadly Neutralizing Epitope in Nonhuman Primates

Graphical Abstract

Highlights

- Env vaccination elicits antibodies that target the V3-glycan-neutralizing epitope

- Repetitive vaccination with a single Env over 4 years induced V3-glycan antibodies

- V3-glycan bnAb precursors recognize Env $Man_9GlcNAc_2$ to neutralize

Authors

Kevin O. Saunders, Nathan I. Nicely, Kevin Wiehe, ..., S. Munir Alam, Samuel J. Danishefsky, Barton F. Haynes

Correspondence

kevin.saunders@dm.duke.edu (K.O.S.), barton.haynes@duke.edu (B.F.H.)

In Brief

Most bnAb epitopes on HIV-1 Envelope include host glycans, but previous Env vaccines have not induced glycan-dependent antibodies. Saunders et al. describe here the ontogeny, crystal structure with glycan, and virion $Man_9GlcNAc_2$-dependent neutralization for glycan-reactive antibodies induced by envelope vaccination.

Accession Numbers

5IIE
5T4Z
KY490540
KY490541
KY490542
KY490543

Vaccine Elicitation of High Mannose-Dependent Neutralizing Antibodies against the V3-Glycan Broadly Neutralizing Epitope in Nonhuman Primates

Kevin O. Saunders,[1,6,16,*] Nathan I. Nicely,[2,6] Kevin Wiehe,[2,6] Mattia Bonsignori,[2,6] R. Ryan Meyerhoff,[3,6] Robert Parks,[2,6] William E. Walkowicz,[7] Baptiste Aussedat,[7] Nelson R. Wu,[2,6] Fangping Cai,[2,6] Yusuf Vohra,[7] Peter K. Park,[7] Amanda Eaton,[1,6] Eden P. Go,[11] Laura L. Sutherland,[2,6] Richard M. Scearce,[2,6] Dan H. Barouch,[14] Ruijun Zhang,[2,6] Tarra Von Holle,[2,6] R. Glenn Overman,[2,6] Kara Anasti,[2,6] Rogier W. Sanders,[13] M. Anthony Moody,[3,5,6] Thomas B. Kepler,[9] Bette Korber,[10] Heather Desaire,[11] Sampa Santra,[8] Norman L. Letvin,[8,15] Gary J. Nabel,[12] David C. Montefiori,[1] Georgia D. Tomaras,[1,3,4,6] Hua-Xin Liao,[2,6] S. Munir Alam,[2,6] Samuel J. Danishefsky,[7] and Barton F. Haynes[2,3,6,*]

[1]Department of Surgery
[2]Department of Medicine
[3]Department of Immunology
[4]Department of Molecular Genetics and Microbiology
[5]Department of Pediatrics
[6]Duke Human Vaccine Institute
Duke University School of Medicine, Durham, NC 27710, USA
[7]Sloan Kettering Institute for Cancer Research, New York, NY 10065, USA
[8]Harvard Medical School, Boston, MA, 02215, USA
[9]Boston University, Boston, MA 02215, USA
[10]LANL, Los Alamos, NM 87545, USA
[11]University of Kansas, Lawrence, KS 66045, USA
[12]Sanofi, Cambridge, MA 02139, USA
[13]Department of Medical Microbiology, Academic Medical Center, University of Amsterdam, 1105 AZ Amsterdam, the Netherlands
[14]Center for Virology and Vaccine Research, Beth Israel Deaconess Medical Center, Boston, MA 02215, USA
[15]Deceased
[16]Lead Contact
*Correspondence: kevin.saunders@dm.duke.edu (K.O.S.), barton.haynes@duke.edu (B.F.H.)
http://dx.doi.org/10.1016/j.celrep.2017.02.003

SUMMARY

Induction of broadly neutralizing antibodies (bnAbs) that target HIV-1 envelope (Env) is a goal of HIV-1 vaccine development. A bnAb target is the Env third variable loop (V3)-glycan site. To determine whether immunization could induce antibodies to the V3-glycan bnAb binding site, we repetitively immunized macaques over a 4-year period with an Env expressing V3-high mannose glycans. Env immunizations elicited plasma antibodies that neutralized HIV-1 expressing only high-mannose glycans—a characteristic shared by early bnAb B cell lineage members. A rhesus recombinant monoclonal antibody from a vaccinated macaque bound to the V3-glycan site at the same amino acids as broadly neutralizing antibodies. A structure of the antibody bound to glycan revealed that the three variable heavy-chain complementarity-determining regions formed a cavity into which glycan could insert and neutralized multiple HIV-1 isolates with high-mannose glycans. Thus, HIV-1 Env vaccination induced mannose-dependent antibodies with characteristics of V3-glycan bnAb precursors.

INTRODUCTION

Development of an effective HIV-1 vaccine is a major goal of HIV-1 prevention strategies (Fauci and Marston, 2014). One objective for an HIV-1 vaccine is to elicit broadly reactive neutralizing antibodies (bnAbs; Burton et al., 2012; Mascola and Haynes, 2013; Mascola and Montefiori, 2010). Broad and potent neutralization of HIV-1 results from antibodies binding to virion-associated trimeric envelope (Env) glycoproteins (Corti and Lanzavecchia, 2013; Parren and Burton, 2001). HIV-1 Env is densely coated with host glycans that provide both a shield against and a target for immune recognition (Doores, 2015; Leonard et al., 1990; Scanlan et al., 2007a; Wei et al., 2003). Most gp120 bnAb epitopes include contacts with glycans (Blattner et al., 2014; Doria-Rose et al., 2014; Garces et al., 2014; Kong et al., 2013; McLellan et al., 2011; Pancera et al., 2014; Pejchal et al., 2011; Zhou et al., 2013), yet Env glycans in the setting of vaccination are poorly immunogenic (Astronomo et al., 2008, 2010; Doores et al., 2010b; Wang et al., 2008). Recent vaccine studies in monkeys, rabbits, and transgenic mice have shown that the presence of glycans alters viral neutralization sensitivity from potently neutralized to resistant (Bradley et al., 2016; Crooks
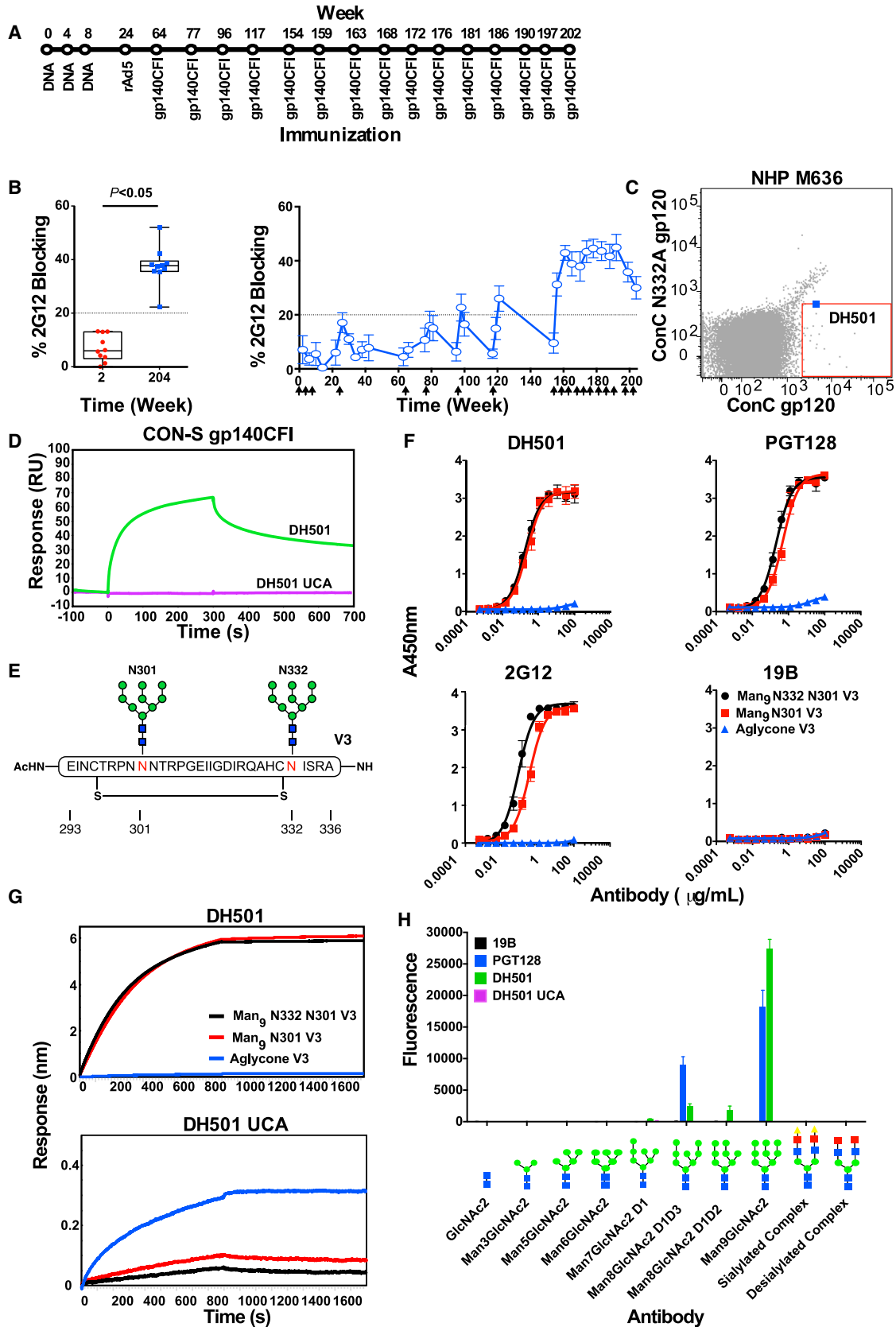
(legend on next page)

et al., 2015; McCoy et al., 2016; Sanders et al., 2015; Tian et al., 2016). Thus, recognition of Env glycans is a major hurdle to HIV-1 vaccine development.

One conserved broadly neutralizing epitope on Env is a patch of high-mannose glycans surrounding the V3 loop (Kong et al., 2013). Human monoclonal bnAbs against the V3-glycan Env site have been isolated from HIV-1-infected individuals, including PGT121, PGT135, and PGT128, which bind N-linked glycans near the V3 loop as well as make contacts with adjacent amino acids (Walker et al., 2011). 2G12 is a neutralizing antibody isolated from natural infection that binds to Env by contacting only the glycans proximal to the V3 loop (Murin et al., 2014). Glycan-targeted antibodies are of particular interest because they are among the most potent bnAbs (Walker et al., 2011) and protect against chimeric simian-human immunodeficiency virus (SHIV) infection in macaques at low plasma concentrations (Moldt et al., 2012).

Here we vaccinated rhesus macaques with a group M consensus Env (M.CON-S gp140CFI) bearing $Man_9GlcNAc_2$ high-mannose glycans on the asparagine at 301 (N301) and the asparagine at 332 (N332) within the V3-glycan site (Go et al., 2008). We show that Env vaccination induced antibodies that blocked the binding of the HIV-1 Env glycan-targeting bnAb 2G12 in ten of ten vaccinated macaques and elicited plasma neutralizing antibodies for viruses with high-density $Man_9GlcNAc_2$ glycans in six of ten macaques. We report the isolation of a vaccine-induced recombinant $Man_9GlcNAc_2$-dependent neutralizing antibody B cell clonal lineage (DH501) that recognized the V3-glycan bnAb epitope and show that both DH501 and V3-glycan bnAb lineage precursors demonstrate $Man_9GlcNAc_2$-dependent neutralization.

RESULTS

Induction of Glycan bnAb-Blocking Antibodies

V3-glycan bnAbs develop in HIV-1-infected individuals only after years of infection (Doria-Rose et al., 2009; Gray et al., 2011; MacLeod et al., 2016; Sather et al., 2009; Simek et al., 2009; Simonich et al., 2016; unpublished data). We asked whether vaccination over a long duration of time with an Env immunogen with N301 and N332 high-mannose glycans (Figures S1A and S1B; Go et al., 2008; Liao et al., 2013b) could elicit glycan-dependent

antibodies. CON-S gp140CFI was chosen for the vaccination because it is glycosylated at the V3 glycan sites with higher percentages of high-mannose glycans than other 293 cell line-derived recombinant Envs such as JR-FL gp140CF (Go et al., 2008). We vaccinated ten rhesus macaques with plasmid DNA encoding M.CON-S gp145, boosted with a recombinant adenovirus serotype 5 viral vector encoding M.CON-S gp145, and further boosted with gp140CFI protein 15 times over 204 weeks (Figure 1A; Figure S1C). We examined plasma antibody responses for their ability to block HIV-1 Env binding of bnAbs 2G12, PGT125, and PGT128, which are dependent on the N-linked glycan at N332 for binding (Figure 1B; Figure S1D). Antibodies that blocked the binding of 2G12 developed in ten of ten animals by week 204 after 15 M.CON-S gp140CFI glycoprotein immunizations (Figure 1B). PGT125 and PGT128 bnAbs were similarly blocked by immune plasma (Figure S1D). However, both PGT125 and PGT128 were blocked by the V3 loop linear peptide monoclonal antibodies (mAbs) 19B and 447-52D (Figure S1E), and, thus, the PGT125 and PGT128 plasma blocking assays were not specific for V3-glycan epitope antibodies. Linear V3 loop antibodies were elicited in the macaques (Figure S1F); thus, the PGT128 blocking could be convoluted by linear V3 loop antibodies. In contrast, the glycan-binding antibody 2G12 was not blocked by V3 loop mAbs (Figure S1E). Therefore, plasma blocking of 2G12 binding to Env was a more precise indicator of glycan-targeted plasma antibody responses than PGT128 or PGT125. Next, we assessed plasma 2G12 blocking over the course of immunization in M.CON-S CFI-vaccinated macaques. DNA priming and rAd5 boost resulted in minimal 2G12 blocking (Figure 1B; Table S1). However, gp140CFI protein immunizations every 8 to 16 weeks increased 2G12-blocking activity, and repetitive gp140CFI boosting every 4 weeks further boosted 2G12 plasma blocking activity (mean peak 2G12 blocking $\pm$ SEM = 45% $\pm$ 5%, n = 10). Thus, plasma blocking of 2G12 suggested that Env-induced antibodies targeting the $Man_9GlcNAc_2$-dependent V3-glycan bnAb epitope were induced.

Isolation of a Rhesus Glycan-Reactive Antibody that Bound the V3-Glycan bnAb Epitope

We next isolated mAbs using antigen-specific memory B cell sorting with fluorophore-labeled consensus Env gp120

Figure 1. Repetitive Vaccination Elicits Antibodies Targeting the V3-Glycan bnAb Epitope

(A) CON-S repetitive vaccination regimen. The immunization modality is shown below the line, and the week of vaccination is noted above the line.

(B) Plasma blocking of 2G12 binding to Env. Left: the percent blocking of 2G12 binding to B.JR-FL gp140C by macaque plasma after one DNA vaccination (week 2) or at the end of the vaccination regimen (week 204; Wilcoxon signed-rank test between weeks 2 and 204, p < 0.05, n = 10). Right: the kinetics of 2G12-blocking antibodies in the plasma of vaccinated macaques. The mean $\pm$ SEM of triplicate measurements is shown (n = 10). Arrows on the x axis indicate vaccination time points.

(C) Fluorescence-activated cell sorting (FACS) plots of sorted single B cells from week 192 peripheral blood mononuclear cells (PBMCs) from CON-S-immunized macaque M636 that bind ConC gp120 but not N332A glycan knockout mutant gp120.

(D) Surface plasmon resonance binding to the study immunogen, CON-S gp140CFI, by DH501 and the DH501 UCA.

(E) Diagram of the $Man_9GlcNAc_2$ glycosylated peptide that recapitulates the PGT128 epitope. N-linked glycans (green and blue) are shown at positions Asn301 (red N) and Asn332 (red N). The disulfide bond is shown with a straight horizontal line.

(F) Direct ELISA binding to the V3 base peptide with $Man_9GlcNAc_2$ glycans at Asn301 and Asn332 (black, Man_9 N332 N301 V3), at Asn301 only (red, Man_9 N301 V3), or at neither site (blue, aglycone) by vaccine-induced macaque antibody DH501.

(G) Biolayer interferometry binding of DH501 and its inferred UCA to the peptides shown in (E).

(H) Glycan luminex detection of antibody binding to 16 μM free glycan. The glycan-dependent bnAb PGT128 and peptide-binding antibody 19B were used as positive and negative controls, respectively. The complex glycan is $Gal_2Man_3GlcNAc_4$.

See also Figures S1 and S2.

(Figure 1C). Antibody DH501 was isolated that used the rhesus *IGHV2* family and had a heavy-chain third complementarity-determining region (CDR-H3) length of 17 amino acids (Table S2). DH501 bound the vaccine immunogen CON-S gp140CFI (Figure 1D) as well as Envs from multiple clades (Figure S2). Somatic mutations were required for binding to CON-S gp140CFI because the inferred unmutated common ancestor (UCA) of DH501 did not bind CON-S gp140CFI (Figure 1D; Figure S2). DH501 binding to M.CON-S gp140CFI was blocked 70% by 2G12 (concentration that inhibits 50% of replication [IC_{50}] = 20 μg/mL; Figure S2B), whereas the peptide-binding V3 antibodies 447-52D and 19B did not block DH501. We determined the ability of DH501 to bind a synthetic glycopeptide with $Man_9GlcNAc_2$ glycans at N301 and N332 (Man_9-V3) that mimics a portion of the gp120 V3-glycan bnAb site (Figure 1E). Both PGT128 and DH501 bound the gp120 V3-glycan minimal antigen (Figures 1F and 1G, top; unpublished data). Like PGT128, DH501 did not bind the aglycone peptide lacking N301 and N332 glycans (Figures 1F and 1G, top). Removal of the glycan at N332 on the glycopeptide and on Env gp120 reduced concentration at half-maximal response (EC_{50}) binding titers 2-fold and 4-fold for PGT128 and 2G12, respectively (Figure 1F), but did not affect DH501 (Figures 1F and 1G, top). Thus, DH501 required the $Man_9GlcNAc_2$ glycan at N301 for binding to the Man_9-V3 glycopeptide. A key question is what Env form bound the DH501 UCA. The DH501 UCA bound both Man_9-V3 glycopeptides and aglycone peptide (Figure 1G, bottom), with strongest binding to the aglycone. This binding pattern was identical to that of the UCA of a V3-glycan bnAb B cell lineage, DH270 (unpublished data). Thus, the DH501 lineage may have been initiated by a denatured Env form or a peptide fragment (Hangartner et al., 2006; Kuraoka et al., 2016).

Similar to PGT128, DH501 bound strongly to free $Man_9GlcNAc_2$ (Figure 1H; Figure S2C; Pejchal et al., 2011). Additionally, DH501 bound weakly to $Man_7GlcNAc_2$ D1, $Man_8GlcNAc_2$ D1D3, and $Man_8GlcNAc_2$ D1D2 (Figure 1H). Conversely, both DH501 and PGT128 did not bind directly to $Gal_2Man_3GlcNAc_4$ complex glycans (Figure 1H). Therefore, terminal mannose residues on all three glycan arms conferred optimal glycan binding by DH501 and PGT128. In contrast to the mutated DH501 antibody, the DH501 UCA did not bind free glycans (Figure 1H; Figure S2C). Expression of Env in cells capable of only high-mannose glycosylation ($GnTI^{-/-}$ cells; Crispin et al., 2006; Eggink et al., 2010; Reeves et al., 2002) improved DH501, PGT128, and 2G12 binding but had no effect on control V3 loop peptide mAb 19B binding (Figure S2D). To express Env with high density of $Man_9GlcNAc_2$ glycans, HIV-1 B.63521 gp140CFI was expressed in the presence of kifunensine (KIF) a glycosylation pathway inhibitor that results in $Man_9GlcNAc_2$ glycosylation (Doores and Burton, 2010; Scanlan et al., 2007b). As a positive control, the binding titer (EC_{50}) of PGT128 to KIF-treated B.63521 Env (0.002 μg/mL) was improved 40-fold compared with PGT128 binding to untreated Env (Figure S2E; Pejchal et al., 2011; Walker et al., 2011). Similar to PGT128, the EC_{50} of DH501 for KIF-63521 Env improved 24-fold compared with DH501 binding to untreated Env (Figure S2E). Thus, DH501 binding to Env was augmented when the glycans on Env were restricted to $Man_9GlcNAc_2$.

DH501 Was Elicited Late during the Vaccination Regimen

We performed competition ELISAs to determine when, during vaccination of macaque M636, antibodies targeting the DH501 epitope were elicited. M636 plasma antibody blocking of DH501 binding to CON-S gp140CFI increased from weeks 156 to 204 of vaccination.

To determine the time of appearance of DH501 clonal lineage B cells, we performed next-generation sequencing (NGS) of the heavy-chain variable region (heavy chain variable region [V_H]) at the beginning of the protein boosts (week 68), after 4 protein boosts (week 117), and after 12 protein boosts (week 188; Figures 2A and 2B). After a single protein boost, there were no DH501 V_H sequences detected (Figure 2B), consistent with the lack of M636 plasma blocking at the same time point (Figures 2A and 2B). Seven DH501 V_H sequences were detected at week 117 after 4 protein boosts. In contrast, 632 sequences were isolated from duplicate sequencing experiments performed on blood B cells after 12 protein boosts at vaccination week 188 (Figure 2B). This late time point corresponded to the time of macaque M636 plasma peak blocking of mAb DH501 binding to Env (Figure 2A).

We clustered the DH501-related sequences to account for the effect of PCR amplification error in NGS sample preparation and examined the genealogy of the resulting NGS sequences. The sequences segregated into two large branches with DH501 appearing in the branch that was the most genetically distant from the UCA (Figure 2C). Three sequences from week 117 and one sequence from week 188 were very similar to the inferred germline antibody of DH501, suggesting that the lineage began at approximately week 117. BnAbs can be limited by immunologic tolerance (Haynes and Verkoczy, 2014); therefore, we determined whether DH501 was autoreactive. DH501 did not bind to host proteins or DNA antigens, nor did it bind to HIV-uninfected HEp-2 cells (Figure S3).

Structural Analysis of Glycan mAb DH501

We determined the structures of the Fab fragment of DH501 in its unliganded state to 2.8-Å resolution (PDB: 5IIE) and in complex with a chemically synthesized, biotinylated $Man_9GlcNAc_2$ molecule to 2.0 Å (PDB: 5T4Z; Figure 3A; Table S3). The mannose residues bound in a pronounced pocket on the paratope of DH501 (Figure 3B). This pocket was formed and bounded by the three variable heavy-chain CDRs. Within the V_H pocket, DH501 primarily contacted the mannose residues with the side-chain functional groups of Asp100E in CDR-H3 and Tyr52 in CDR-H2. Additional stabilization of the complex was established with contacts between the mannose residues and the polypeptide backbone of residues Gly100A and Tyr100C in CDR-H3 as well as through water H bonds to the Thr100D side chain and the carbonyl of Gly100A in CDR-H3. Interestingly, the structure indicated that the most proximal mannose residue had to be a terminal one on the $Man_9GlcNAc_2$ molecule because the electron density was well defined, and the structure showed no room for another mannose residue. The electron density for the most distal mannose residue was not as well defined but best corresponded with an alpha1-3 linkage, indicating that the mannose residues were from the D2 arm of the synthesized $Man_9GlcNAc_2$ compound.
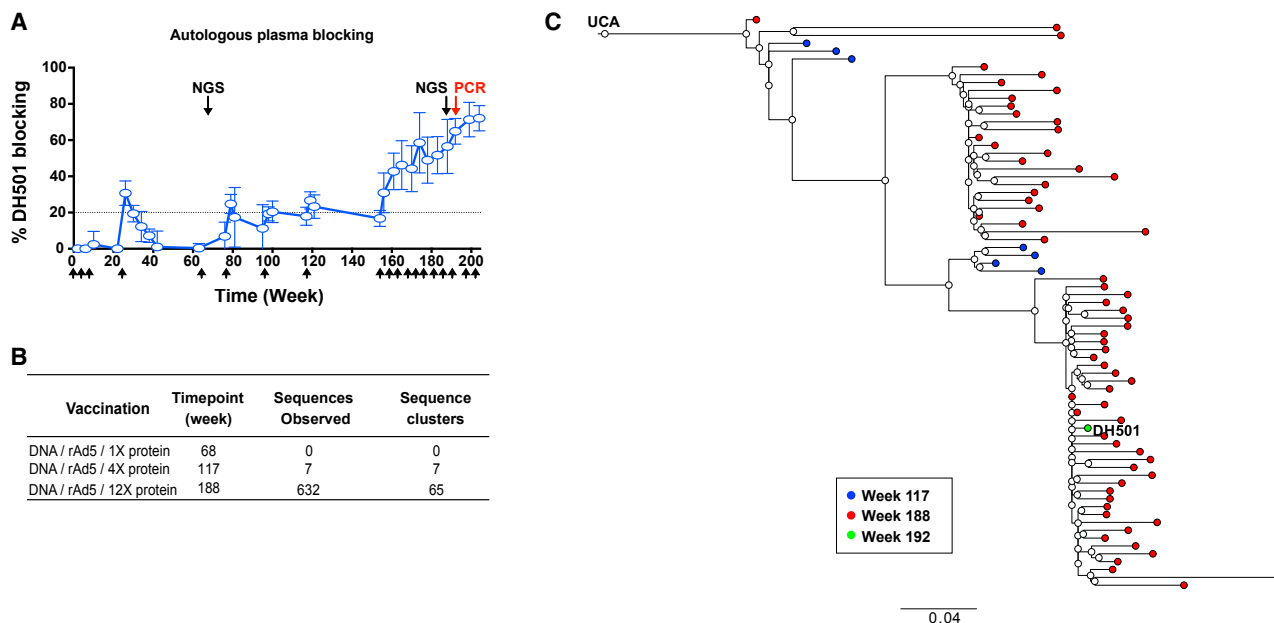
Figure 2. Genetic and Plasma Analyses Determine that DH501 Was Elicited after Multiple Protein Boosts

(A) Autologous plasma blocking of DH501 binding to the CON-S immunogen. The plasma from sequential time points from macaque M636 from whom the DH501 glycan-reactive antibody was isolated was used to block DH501 binding to Env. Time points where next-generation sequencing was performed in (B) are indicated by black arrows. The red arrow indicates where DH501 was isolated by single B cell sorting and RT-PCR. Values greater than 20% are considered positive. The mean ± SEM of triplicate measurements is shown (n = 10). Arrows on the x axis indicate vaccination time points.

(B) Comparison of the number of DH501-related sequences after DNA prime, rAd5 boost, and one protein boost, four protein boosts, or 12 protein boosts in macaque M636, from which DH501 was cloned. Sequencing was performed twice at each time point, and DH501 clonal relatedness was determined using Clonanalyst (second column). Sequences were clustered to account for sequencing errors. The number of sequence clusters represents the estimated minimum number of DH501 members at each time point (last column).

(C) The maximum likelihood phylogenetic tree of the 73 total collapsed sequences (72 from NGS and DH501) that are clonally related to DH501. The time point at which the sequence was observed is indicated by the color code at the bottom.

See also Figure S3.

The DH501 Fab structure was compared with known liganded structures of gp120 V3-glycan antibodies: PGT122 (PDB: 4NCO; Julien et al., 2013), PGT124 (PDB: 4R2G; Garces et al., 2014), PGT128 (PDB: 3TYG; Pejchal et al., 2011), and PGT135 (PDB: 4JM2; Kong et al., 2013). In direct contrast to PGT128, which had long CDR-H2 and -H3 in extended conformations, DH501 had shorter CDRs (Figure 3C). More generally, these shorter CDRs distinguished DH501 from the broadly neutralizing antibodies PGT128 and PGT135 because they all had heavy-chain CDR insertions (Walker et al., 2011). Structurally, the long CDRs with extended conformations were able to penetrate the glycan shield to contact the gp120 polypeptide (Figures 3D and 3E; Doores et al., 2015; Kong et al., 2013; Pejchal et al., 2011; Walker et al., 2011). When DH501 was superimposed on the structure of PGT122 binding to gp120 or the BG505 SOSIP.664 trimer, it was evident that the 26-amino acid CDR-H3 of PGT122 made contacts with the Env trimer that DH501 would be less capable of making because of its shorter 17 amino acid CDR-H3 (Figure 3E). However, despite these differences in CDR lengths and conformations, the DH501 Fab bound the near-native, closed BG505 SOSIP.v4.1 trimer (K_d = 0.31 μM; Figure 3F; de Taeye et al., 2015).

When the electrostatic surface potentials of the paratopes of DH501 and other V3 glycan antibody structures were compared,

DH501 exhibited a large, negatively charged region overlapping with the glycan-binding pocket (Figure 4). The strong negative charge in the vicinity of the pocket was due to an Asp54-Asp55 doublet in CDR-H2 as well as nearby Glu57. Within the pocket itself, the negative charge was driven by the side chains of Tyr52 and Asp100E (Figure S4). This charged pocket provided a favorable environment for interacting with mannose residues in contrast to the other V3 glycan antibodies that showed broader surface features and, instead, used their long CDRs to establish more interfaces with the glycoprotein.

DH501 Neutralization of HIV-1

We produced B.JR-FL, A.BG505, and AE.CNE8 pseudoviruses in KIF to generate pseudoviruses enriched for a high density of $Man_9GlcNAc_2$ glycosylation (KIF-JRFL, KIF-BG505, and KIF-CNE8). We found that plasma gamma immunoglobulin (IgG) from six of ten macaques neutralized at least one KIF-treated tier 2 virus, whereas none were able to neutralize the corresponding untreated tier 2 pseudoviruses (Figure S5A). However, the plasma did have relatively high titers of neutralizing antibodies against untreated, easy-to-neutralize tier 1 pseudoviruses (Figure S5B). We produced seven additional pseudoviruses in KIF-treated cells and tested neutralization by DH501 and its inferred UCA. The DH501 mAb neutralized ten of
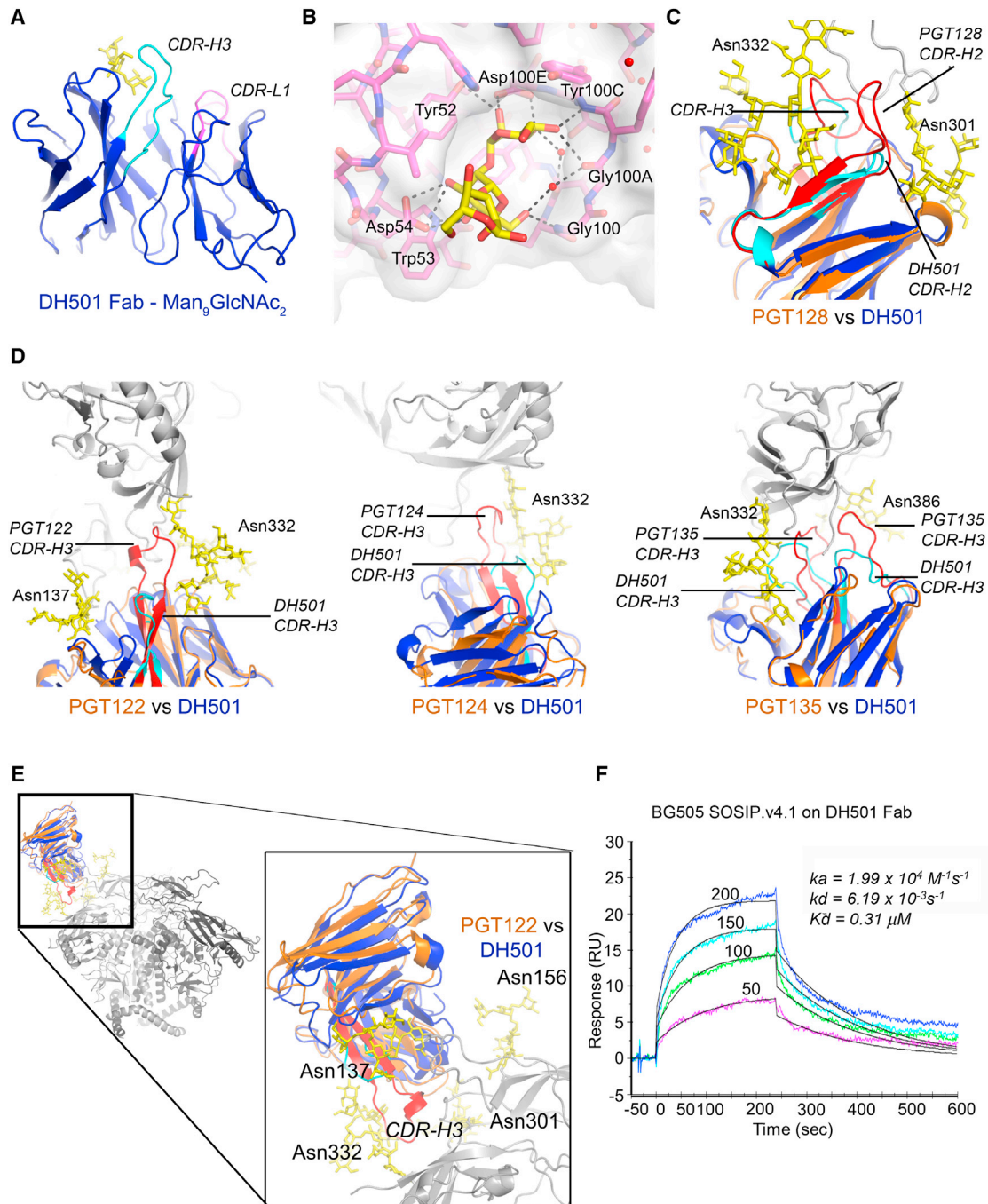
Figure 3. The Molecular Basis for High-Mannose and Env Recognition by DH501

(A) The structure of DH501 Fv (blue) with the paratope oriented upward. CDR-H3 is highlighted in cyan, CDR-L1 in magenta, and bound constituents of the $Man_9GlcNAc_2$ compound in yellow.

(B) Specific interactions between DH501 (magenta carbons behind a surface rendering) and bound mannose residues (yellow carbons). H-bonding interactions are shown with dashed lines, and interacting residues on the DH501 heavy chain are labeled.

(C) DH501 Fv (color scheme as in A) superimposed with PGT130 Fv in orange with its CDR-H3 in red and CDR-L1 in green.

(D) DH501 Fv superimposed with the Fvs of V3-glycan broadly neutralizing antibodies in complex with gp120. Gp120 and glycan moieties are shown in gray and yellow, respectively. DH501 is colored as in (A), and compared antibodies are shown in orange. Long CDRs with extended conformations in V3 glycan bnAbs are highlighted in red. N-linked Asn residues are numbered for identification of glycans.

ten KIF-treated pseudoviruses (geometric mean titer IC_{50} = 0.34 μg/mL) but none of the untreated pseudoviruses (Figure 5A). Neutralization activity was acquired with somatic mutation because the DH501 UCA did not neutralize any of the KIF-treated or untreated viruses (Figure 5A). As controls, KIF-treated pseudoviruses were more sensitive to PGT128 neutralization and more resistant to PG9 (V1V2 bnAb) neutralization than untreated pseudoviruses (Figure 5A; Walker et al., 2009, 2011). Importantly, difficult-to-neutralize (tier 2) viruses remained tier 2 in neutralization sensitivity after KIF treatment (Table S4). Interestingly, KIF-B.MN was the weakest neutralized pseudovirus and lacked N301, whereas all remaining viruses in the panel had an asparagine at position 301 (Figure S5C).

DH501 Targets V3 Glycans and the Base of the V3 Loop for HIV Neutralization

To determine the glycans required for DH501 neutralization, we eliminated the N-linked glycosylation sites at Env amino acids 295, 301, 332, 386, or 392 in B.JR-FL by mutating asparagine to alanine at each of these positions. DH501 neutralized all KIF-JR-FL mutant viruses equivalently, except the N301A mutant, for which neutralization was abrogated (Figure 5B). The N301 glycan was also necessary for neutralization of KIF-JR-FL by PGT128 (Figure 5B), consistent with its interaction with this glycan in the crystal structure of PGT128 in complex with the B.JR-FL outer domain (Pejchal et al., 2011). However, DH501 neutralized KIF-JR-FL N332A, whereas PGT128 showed a decrease in potency for neutralization of KIF-JR-FL N332A (Figure 5B). Thus, like Man9-V3 glycopeptide binding (Figures 1F and 1G), DH501 relied only on N301 for neutralization of KIF-JR-FL.

Most of the V3-glycan bnAbs contact the highly conserved amino acids Gly324, Asp325, Ile326, and Arg327 (GDIR motif) at the base of the V3 loop (Garces et al., 2014; Pejchal et al., 2011; Sok et al., 2016). Mutating Gly324 (ADIR) ablated neutralization of KIF-JRFL by both DH501 and PGT128 (Figure 5C). Asp325 and Arg327 were required by PGT128 for potent neutralization of KIF-JRFL when mutated singularly (GAIR) or in tandem (GAIA). These two residues were also required by DH501 for neutralization when mutated in tandem (Figure 5C). Thus, like known V3-glycan bnAbs, DH501 neutralization of KIF-treated viruses was not only N301 glycan-dependent but also relied on amino acid residues within the GDIR motif of the base of the V3 loop.

V3 Glycan bnAb Lineage Precursors Require Man9GlcNAc2 for Heterologous Neutralization

The significance of antibodies that neutralize kifunensine-treated viruses is a critical question. Thus, we examined the requirement for Man9GlcNAc2 glycosylation for neutralization susceptibility during the development of a V3-glycan bnAb lineage, DH270 (Figure 5D; unpublished data). The DH270 bnAb lineage is

N332 and N301 glycan-dependent and requires the GDIR motif for binding (unpublished data). The DH270 UCA did not neutralize either untreated B.JR-FL or KIF-JR-FL (Figure 5D). Similar to DH501, the first DH270 B cell lineage intermediate antibody IA4 neutralized KIF-JR-FL (IC_{50} = 8.73 μg/mL) but not the untreated B.JR-FL pseudovirus. The intermediate antibodies IA2 and IA3 neutralized KIF-JR-FL 5-fold and 10-fold more potently compared with untreated B.JR-FL, respectively. B.JR-FL neutralization by more mutated DH270 bnAb lineage antibodies was less affected by kifunensine treatment (Figure 5D). Thus, like DH501, precursors in the V3-glycan bnAb lineage required a high density of Man9GlcNAc2 for HIV-1 B.JR-FL neutralization, whereas affinity-matured V3-glycan bnAbs acquired the ability to neutralize B.JR-FL regardless of virus high-mannose glycan enrichment.

DISCUSSION

Here we have demonstrated that Man9GlcNAc2-dependent Env antibodies can be induced in the setting of vaccination with Envs glycosylated with V3 Man9GlcNAc2 glycans. Several groups have attempted to elicit 2G12-like antibodies using BSA conjugated to high-mannose (Astronomo et al., 2008), phage-bearing high-mannose (Astronomo et al., 2010; Doores et al., 2010b), or synthetic glycopeptides (Joyce et al., 2008). However, these studies were unable to produce 2G12-like antibodies, perhaps because of the domain swap within 2G12 (Calarese et al., 2003), lack of immunogenicity of host glycans (Scanlan et al., 2007b), or the lack of high mannose glycosylation on recombinant 293 cell line-produced gp120 and cleavage-deficient non-SOSIP gp140 immunogens (Bonomelli et al., 2011; Doores et al., 2010a; Go et al., 2008). In a recent study, one of 15 rabbits immunized with an Env trimer had a reduction in neutralization potency when the N332 glycan site was deleted on HIV-1 Env (Sanders et al., 2015). The rarity of V3-glycan-dependent antibodies elicited by vaccination has raised the question of whether Env high-mannose glycans are immunogenic (Scanlan et al., 2007a). Mannose is a component of the cell wall of fungal pathogens to which the human immune system has evolved to make antibodies (Deshaw and Pirofski, 1995); however, the recognition of the precise arrangement of mannose and the accommodation or avoidance of complex glycans on Env may be an obstacle for eliciting HIV-1 Env glycan antibodies (Garces et al., 2015). Anti-fungal antibodies have been induced in rabbits that neutralize HIV-1 produced in kifunensine (Agrawal-Gamse et al., 2011; Dunlop et al., 2010; Zhang et al., 2015), but whether these antibodies target bnAb epitopes such as the N332 glycan or require the GDIR motif is unknown. Furthermore, our study shows that the significance of kifunensine-dependent neutralization is that when V3 glycan bnAb lineages are initiated in HIV-1 infection, bnAb precursors require Man9GlcNAc2 Env glycosylation for heterologous neutralization and evolve with affinity

(E) DH501 Fv (blue) superimposed on PGT122 Fv (orange) bound to the BG505.6R.SOSIP.664 trimer (gray). DH501's CDR-H3 (cyan) lacks the length of the PGT122s CDR-H3 (red) to deeply penetrate the glycan shield (yellow).
(F) SPR binding of the DH501 Fab to a stabilized BG505 SOSIP.v4.1 trimer. Each trace represents a different concentration of Fab ranging from 50 to 200 μg/mL as indicated. The affinity measurements are displayed in the right corner of the graph.
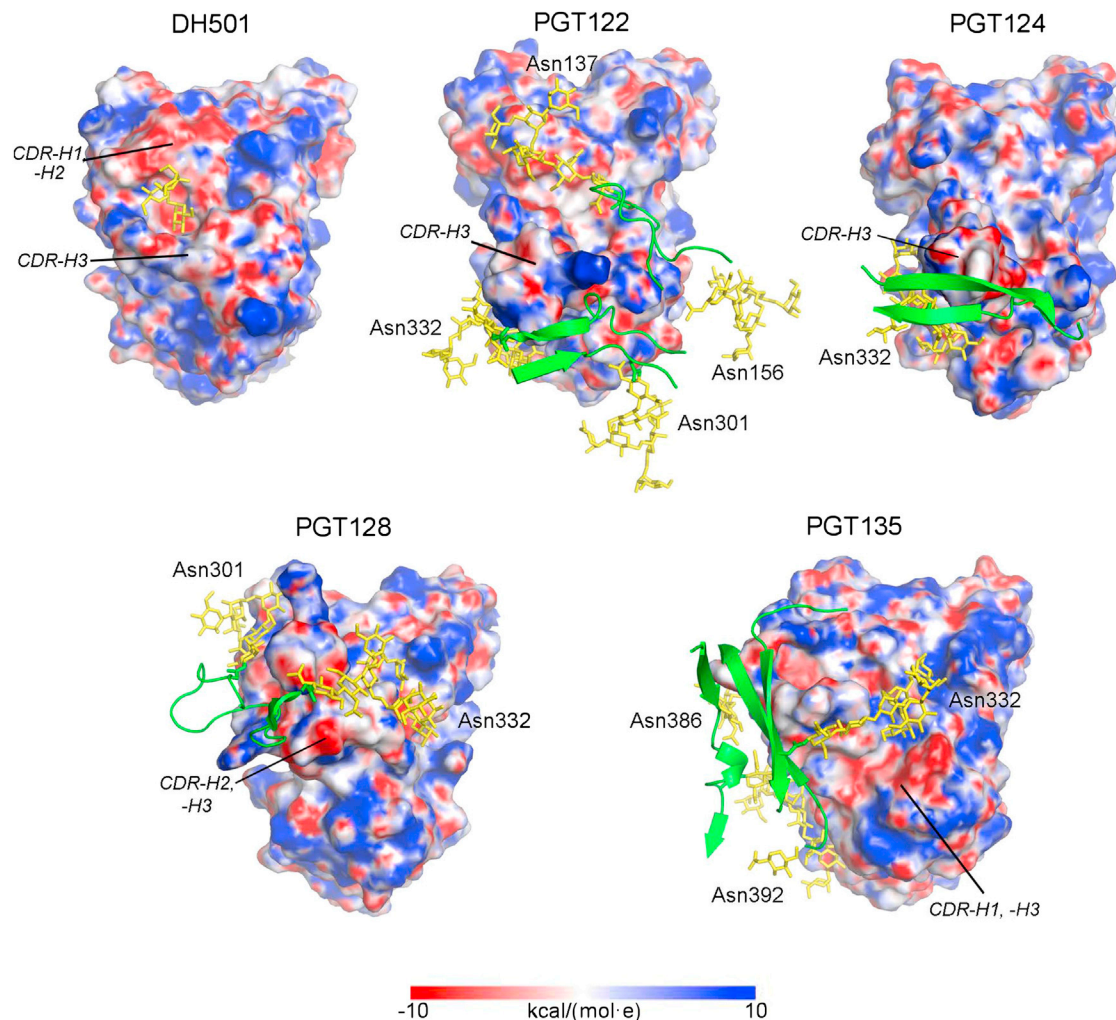See also Figure S4.

Figure 4. DH501 Accommodates High-Mannose Glycan by Forming a Negatively Charged Glycan-Binding Pocket

Shown are paratope surfaces rendered by electrostatic surface potential along with gp120 and labeled glycans in green and yellow, respectively. The electrostatic potential surface renderings were calculated using Chemistry at Harvard Macromolecular Mechanics (CHARMM; Im et al., 1998; Jo et al., 2008a, 2008b) and expressed in units of kcal/(mol·e). The paratope is shown from a top view, with the heavy chains oriented at the top and light chains at the bottom. CDRs with extended conformations protruding from the paratope surface are labeled in italics. V3-glycan bnAbs were characterized by one or more long CDRs and an amphipathic charge distribution. DH501 is distinguished by a pronounced pocket on its paratope bordered and formed almost entirely by the three heavy-chain CDRs. The mannose residues of $Man_9GlcNAc_2$ that bind within the pocket are shown in yellow.

maturation to be less dependent on a high density of $Man_9GlcNAc_2$. Structural studies of the PGT121 family have shown that, as antibodies evolve, they acquire binding mechanisms to avoid or accommodate interfering glycans (Garces et al., 2015). Although the ability to neutralize KIF-treated HIV is a trait of early V3-glycan bnAb precursors, it should be emphasized that not all antibodies like DH501 that neutralize KIF-treated HIV may have the capacity to affinity-mature to full bnAb breadth. Thus, the only way to definitively know whether DH501 is on the path to become an bnAb is to isolate a DH501-like, affinity-matured bnAb, and work is underway to seek such antibodies.

The mode of glycan recognition by DH501 is distinct from bnAbs like PGT121 or PGT128, which use long loops in extended conformations to contact glycans (Figure 3). The lack of these long, extended loops and, instead, the presence of a glycan-binding pocket is compatible with a scenario in which the glycan inserts into the cavity, allowing DH501 to move proximal to the peptide backbone and, thereby, contact the GDIR motif.

How to increase the neutralization breadth of vaccine-induced antibodies like DH501 is a key question. Superpositions of DH501 with V3-glycan bnAbs demonstrated that DH501 lacked the protruding CDR loops created by insertions (Figures 3C and 3D; Figure S4). Insertions and deletions are common in V3-glycan bnAbs (Walker et al., 2011) but are events rarely found in the antibody repertoire (Kepler et al., 2014) and may represent a roadblock to bnAb induction. The removal of the insertion in the CDR-H2 of PGT128 diminished its neutralization potency and
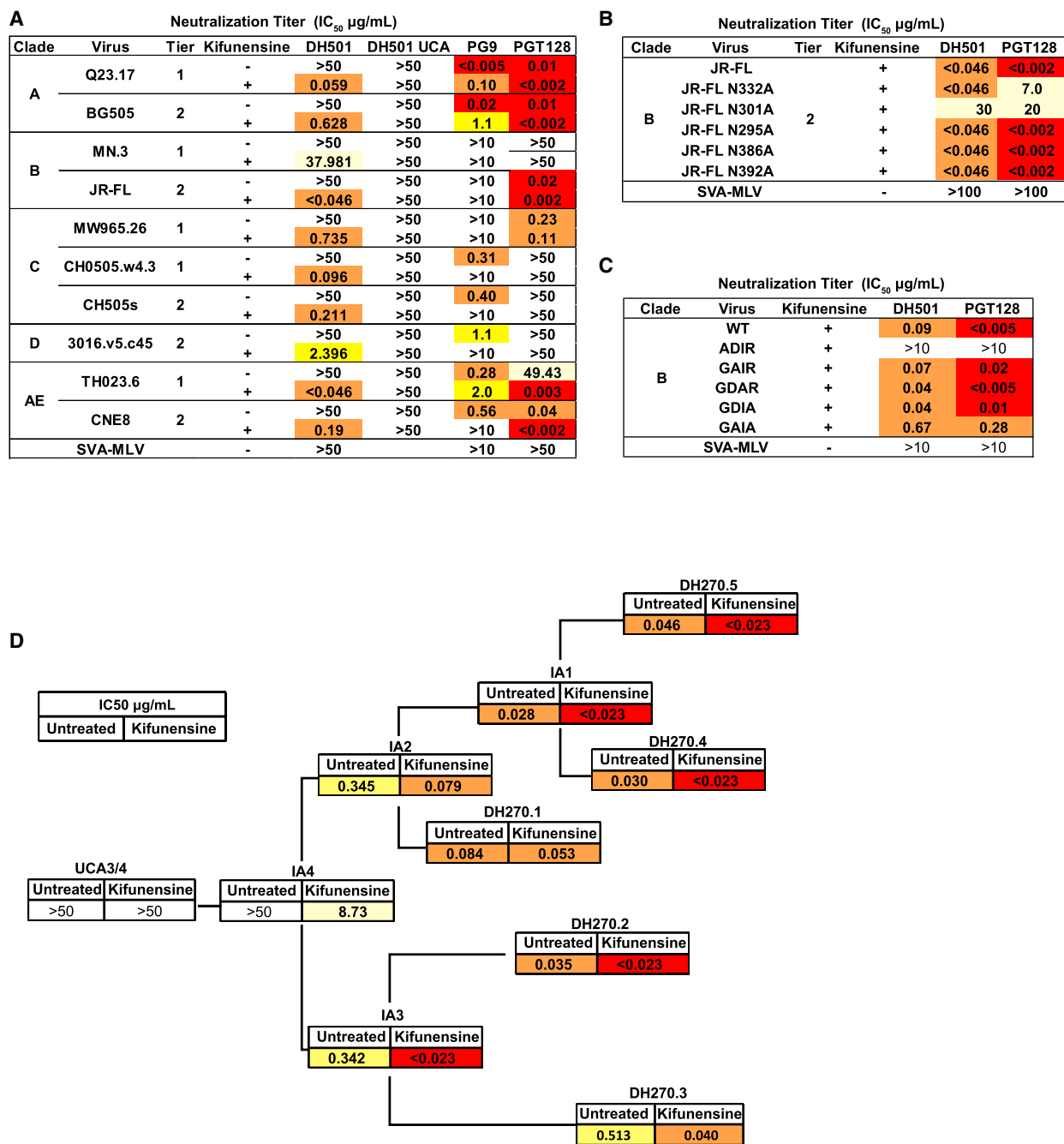
A

Neutralization Titer (IC$_{50}$ µg/mL)

Clade	Virus	Tier	Kifunensine	DH501	DH501 UCA	PG9	PGT128
A	Q23.17	1	-	>50	>50	<0.005	0.01
			+	0.059	>50	0.10	<0.002
	BG505	2	-	>50	>50	0.02	0.01
			+	0.628	>50	1.1	<0.002
B	MN.3	1	-	>50	>50	>10	>50
			+	37.981	>50	>10	>50
	JR-FL	2	-	>50	>50	>10	0.02
			+	<0.046	>50	>10	0.002
C	MW965.26	1	-	>50	>50	>10	0.23
			+	0.735	>50	>10	0.11
	CH0505.w4.3	1	-	>50	>50	0.31	>50
			+	0.096	>50	>10	>50
	CH505s	2	-	>50	>50	0.40	>50
			+	0.211	>50	>10	>50
D	3016.v5.c45	2	-	>50	>50	1.1	>50
			+	2.396	>50	>10	>50
AE	TH023.6	1	-	>50	>50	0.28	49.43
			+	<0.046	>50	2.0	0.003
	CNE8	2	-	>50	>50	0.56	0.04
			+	0.19	>50	>10	<0.002
SVA-MLV			-	>50		>10	>50

B

Neutralization Titer (IC$_{50}$ µg/mL)

Clade	Virus	Tier	Kifunensine	DH501	PGT128
B	JR-FL	2	+	<0.046	<0.002
	JR-FL N332A		+	<0.046	7.0
	JR-FL N301A		+	30	20
	JR-FL N295A		+	<0.046	<0.002
	JR-FL N386A		+	<0.046	<0.002
	JR-FL N392A		+	<0.046	<0.002
SVA-MLV			-	>100	>100

C

Neutralization Titer (IC$_{50}$ µg/mL)

Clade	Virus	Kifunensine	DH501	PGT128
B	WT	+	0.09	<0.005
	ADIR	+	>10	>10
	GAIR	+	0.07	0.02
	GDAR	+	0.04	<0.005
	GDIA	+	0.04	0.01
	GAIA	+	0.67	0.28
SVA-MLV		-	>10	>10

D

Figure 5. DH501 and Early V3 Glycan bnAb Lineage Antibodies Require Man$_9$GlcNAc$_2$ Glycosylation for Neutralization of HIV-1

(A) Neutralization titers against a cross-clade panel of tier 1 and tier 2 viruses in the TZM-bl assay. Each virus was produced untreated or treated with kifunensine. PG9 (Man$_5$GlcNAc2-reactive) and PGT128 (Man$_9$GlcNAc$_2$-reactive) were used as controls to demonstrate the modification of envelope glycosylation on virions. Representative titers are shown from up to four independent assays.

(B) DH501 exhibits N301-dependent neutralization of kifunensine-treated B.JRFL. Shown is neutralization of kifunensine-treated B.JR-FL (KIF-JR-FL) with intact wild-type N-linked glycosylation sites or with an alanine substitution at the indicated glycosylation site. SVA is a murine leukemia virus used as a negative control for neutralization. Values are the geometric mean for two independent experiments.

(C) DH501 requires the GDIR motif for neutralization of kifunensine-treated B.JRFL. Shown are TZM-bl neutralization titers (IC$_{50}$, micrograms per milliliter) for DH501 and PGT128 against wild-type and GDIR alanine mutant viruses produced in kifunensine-treated cells.

N332 glycan dependence (Doores et al., 2015; Pejchal et al., 2011), supporting the notion that insertion and deletions may be required for optimal neutralization breadth. Future studies will aim to induce activation induced cytidine deaminase (AID)-mediated insertions and deletions by vaccinating under conditions that promote AID activity (Bowers et al., 2014). Also, 2G12 did not block 100% of DH501 binding to Env, which could be due to DH501 requiring the N301 glycan more than the N332 glycan. The N332 glycan is one of the most abundantly targeted sites on Env for broadly neutralizing antibodies in sera (Walker et al., 2010). Whether N301 glycan recognition alone is sufficient to confer broad neutralization is unknown.

To select V3-glycan antibodies that mature during vaccination into broadly neutralizing antibodies will likely require a sequential Env vaccination regimen (Bonsignori et al., 2016; Escolano et al., 2016; Haynes et al., 2012; Liao et al., 2013a; unpublished data). Synthetic peptides from the base of the V3 loop that bound to the DH501 UCA (Figure 1G) and the DH270 UCA could prove useful as germline-targeting immunogens to initiate V3-glycan bnAb antibodies. This peptide, although it contains a disulfide bond to link the N and C terminus, providing a conformation similar to the base of the V3 loop, and binds to the UCA, may not be optimal for induction of conformational Env antibodies unless the disulfide-bonded loop is sufficient for this purpose. The peptide does not contain the tip of the V3 loop that is immunogenic for non-neutralizing antibodies but, instead, includes the base of the V3 loop that contains the GDIR motif that is bound by many V3-glycan bnAbs (Garces et al., 2014, 2015; Kong et al., 2013). Priming immunizations with the V3 base peptide may be more beneficial than priming with a gp140 because the UCA of the V3-glycan bnAb DH270 did not bind to the N332 and N301 glycan-deleted gp140 but did bind to the aglycone V3 base peptide (unpublished data). This difference in binding could be due to the V1V2 loop and its glycans shielding the base of the V3 loop in the context of gp140 (Steichen et al., 2016; unpublished data). It will be of interest to study this peptide in DH270 UCA VH and light chain variable region (VL) bnAb knockin mice to determine the usefulness of the peptide as an immunogen. Subsequent boosts could include repetitive vaccination with sequential Envs from HIV-1-infected individuals who develop V3-glycan bnAbs that have been expressed with only $Man_9GlcNAc_2$ because we show here that the earliest bnAb lineage members require $Man_9GlcNAc_2$ for recognition of the trimer (Escolano et al., 2016; MacLeod et al., 2016; unpublished data). Additionally, many bnAbs are limited by immunologic tolerance (Haynes and Verkoczy, 2014); therefore, relaxing tolerance while vaccinating may also be necessary for bnAb induction. Relaxation of tolerance controls coupled with the types of regimens described above could shorten the time needed to elicit V3-glycan antibodies compared with the study described here.

However, immunization occurs yearly with influenza and, thus, may also be possible for HIV-1 vaccines. Vaccination of infants and continued boosts throughout life may also be a plausible method for repetitively vaccinating against HIV-1 in high-risk populations. Nonetheless, the results presented here demonstrate that induction of antibodies targeting the V3-glycan bnAb epitope with an Env expressing $Man_9GlcNAc_2$ glycans at the base of the V3 loop is possible with repetitive immunizations and represent a first step in the induction of V3-glycan-targeted neutralizing antibody B cell lineages in primates.

EXPERIMENTAL PROCEDURES

Experimental Design

Indian-origin rhesus macaques (n = 10) were administered CON-S gp145 or gp140CFI as described in Figure 1A and the Supplemental Experimental Procedures. Indian-origin rhesus macaques were housed in an Association for Assessment and Accreditation of Laboratory Animal Care (AAALAC)-accredited facility, and all procedures were conducted with Institutional Animal Care and Use Committee (IACUC) approval.

Oligomannose Bead Immunoassay

Antibody binding to free glycan was measured by a custom glycan luminex microsphere assay as detailed in the Supplemental Experimental Procedures.

Surface Plasmon Resonance Detection of Antibody Binding to gp140

Binding of CON-S gp140CFI (100 mg/mL) or BG505 SOSIP.664.v4.1 gp140 (228 nM to 913 nM) was measured by surface plasmon resonance (SPR) (BIAcoreS200, GE Healthcare) analysis following capture of each mAb on anti-human Ig Fc immobilized or direct immobilization of Fabs on sensors as described earlier (Alam et al., 2013).

$Man_9GlcNAc_2$-V3 Glycopeptide and Aglycone Bio-layer Interferometry

Antibody binding to biotinylated synthetic glycopeptide was measured by bio-layer interferometry (BLI, ForteBio Octet Red96) analysis.

Direct ELISAs

ELISA plates were coated with antigen, blocked, and incubated with serially diluted antibodies. Biotinylated antigens were captured with streptavidin. Bound antibody was detected with anti-human IgG (Rockland) or an anti-rhesus IgG conjugated to horseradish peroxidase (HRP). HRP was detected with tetramethylbenzidine (TMB) (KPL) and read with a SpectraMax plate reader (Molecular Devices) and SoftMax Pro v5.3 (Molecular Devices). See also Supplemental Experimental Procedures.

Plasma and Antibody Blocking of N332 Glycan-Dependent bnAb

B.JRFL gp140C-coated plates were incubated sequentially with blocking plasma or blocking antibody, followed by addition of biotinylated antibodies of interest. Binding in the presence of competitor was compared with binding in the absence of the competitor antibodies to determine percent blocking. See also Supplemental Experimental Procedures.

Epitope-Specific Single B Cell Sorting

B cell sorting was performed as described previously (Wiehe et al., 2014) with fluorophore-labeled ConC gp120 and ConC N332A gp120 as stated in the Supplemental Experimental Procedures.

(D) Neutralization of B.JR-FL and KIF-JR-FL pseudovirus by the broadly neutralizing N332 glycan-dependent DH270 lineage antibodies. Neutralization titer is shown as IC_{50} (micrograms per milliliter). The IC_{50} for B.JR-FL neutralization is shown in the first column, followed by the KIF-JR-FL neutralization titer. Neutralization titers are color coded as >50 (white), 49–1 (light yellow), 0.9–0.1 (yellow), 0.09–0.023 (orange), and <0.023 (red). Titers are the geometric mean of two independent experiments.
See also Figure S5.

Rhesus Immunoglobulin RT-PCR

Immunoglobulin genes were amplified as described previously (Liao et al., 2009; Wiehe et al., 2014). Contigs of the PCR amplicon sequence were made, and genes were inferred with the human library in Somatic Diversification Analysis software (SoDA) and the rhesus library in Clonanalyst (Volpe et al., 2006; Wiehe et al., 2014). Unmutated common ancestor antibodies were inferred using the rhesus library in Clonanalyst. Antibodies were expressed as described in Zhang et al., 2016.

Next-Generation Sequencing of Antibody Genes

Illumina MiSeq sequencing of antibody heavy-chain variable, diversity, joining (VDJ) sequences was performed on peripheral B cells as described previously (Zhang et al., 2016). For each time point, sequencing was performed twice on independent cDNA samples to confirm the absence or presence of antibody sequences of interest. From single template NGS experiments, we have observed that the number of errors introduced in PCR amplification in our NGS sample preparation rarely exceeds four base pairs (<1%). Thus, two sequences that each differ by four base pairs (eight total base pair differences) cannot be reliably determined to derive from two unique B cells. To conservatively account for this, we clustered together sequences with eight or fewer base pair differences. V, D, and J gene segment inference, clonal relatedness testing, and reconstruction of clonal lineage trees were performed using the Clonanalyst software package (Kepler, 2013).

HEp-2 Cell Immunofluorescence

Rhesus antibodies were tested at 25 and 50 μg/mL in the HEp-2 cell immunofluorescence assay (Inverness Medical Professional Diagnostics) as described previously (Moody et al., 2012).

Recombinant Env Expression

Recombinant Env was produced in 293F cells by transient transfection as described in the Supplemental Experimental Procedures. BG505 SOSIP.v4.1 trimers were purified using PGT145 affinity chromatography as described previously (de Taeye et al., 2015).

Glycosylation Analysis

Glycan analysis was performed by liquid chromatography-tandem mass spectrometry (LC-MS/MS) as described previously (Go et al., 2013, 2015). See also Supplemental Experimental Procedures.

In Vitro HIV-1 Neutralization

Neutralizing antibody activity was measured in 96-well culture plates by using Tat-regulated luciferase (Luc) reporter gene expression to quantify reductions in virus infection in TZM-bl cells.

Crystallography

Crystallization conditions were tested in a variety of commercially available screens (QIAGEN, Hampton Research), and crystals of the unliganded Fab were observed over a reservoir of 0.1 M HEPES (pH 6.5), 20% polyethylene glycol (PEG) 6000 at a temperature of 20°C. Purified DH501 Fab was also mixed with $Man_9GlcNAc_2$-biotin in a 1:3 molar ratio and then treated to the same procedure as the unliganded Fab. Crystals were observed over a reservoir of 0.2 M $CaCl_2$, 20% PEG 3350. Coordinates and structure factors have been deposited in the PDB under accession codes 5IIE (unliganded Fab) and 5T4Z (liganded Fab). Structural figures were generated with Pymol (DeLano, 2012). Further details can be found in the Supplemental Experimental Procedures.

Statistical Analysis Plan

Descriptive statistics were used to describe immune responses. Neutralization data were averaged across experiments as geometric means. A Wilcoxon signed-rank test was performed, including all ten animals, to compare differences in plasma blocking at two different time points. Statistics were calculated with SAS v9.4.

ACCESSION NUMBERS

The accession numbers for the coordinates and structure factors for the DH501 unliganded Fab and the Fab-Man9GlcNAc2 complex reported in this paper are PDB: 5IIE and 5T4Z. The accession numbers for the sequence of DH501 heavy and light chain reported in this paper are GenBank: KY490540 and KY490541. The accession numbers for the sequence of DH501 unmutated common ancestor heavy and light chain reported in this paper are GenBank: KY490542 and KY490543.

SUPPLEMENTAL INFORMATION

Supplemental Information includes Supplemental Experimental Procedures, five figures, and four tables and can be found with this article online at http://dx.doi.org/10.1016/j.celrep.2017.02.003.

AUTHOR CONTRIBUTIONS

Conceptualization, K.O.S. and B.F.H.; Investigation, K.O.S., N.I.N., N.R.W., A.F., M.B., R.R.M., K.A., E.G., W.E.W., B.A., Y.V., P.K.P., R.W.S., F.P.C., R.Z., T.V.H., R.P., R.G.O., A.E., D.B., S.S., L.L.S., R.S., and B.T.K.; Writing, K.O.S. and B.F.H.; Supervision, B.F.H., K.O.S., M.B., G.D.T., S.M.A., S.J.D., M.A.M., D.C.M., H.X.L., G.J.N., and N.L.L.; Funding Acquisition, K.O.S. and B.F.H.; Formal Analysis, K.O.S., N.I.N., K.W., E.G., H.D., R.G.O., T.B.K., and B.F.H.; Software, T.B.K.

REFERENCES

Agrawal-Gamse, C., Luallen, R.J., Liu, B., Fu, H., Lee, F.H., Geng, Y., and Doms, R.W. (2011). Yeast-elicited cross-reactive antibodies to HIV Env glycans efficiently neutralize virions expressing exclusively high-mannose N-linked glycans. J. Virol. 85, 470–480.

Alam, S.M., Dennison, S.M., Aussedat, B., Vohra, Y., Park, P.K., Fernández-Tejada, A., Stewart, S., Jaeger, F.H., Anasti, K., Blinn, J.H., et al. (2013). Recognition of synthetic glycopeptides by HIV-1 broadly neutralizing antibodies and their unmutated ancestors. Proc. Natl. Acad. Sci. 110, 18214–18219.

Astronomo, R.D., Lee, H.K., Scanlan, C.N., Pantophlet, R., Huang, C.Y., Wilson, I.A., Blixt, O., Dwek, R.A., Wong, C.H., and Burton, D.R. (2008). A glycoconjugate antigen based on the recognition motif of a broadly neutralizing human immunodeficiency virus antibody, 2G12, is immunogenic but elicits antibodies unable to bind to the self glycans of gp120. J. Virol. 82, 6359–6368.

Astronomo, R.D., Kaltgrad, E., Udit, A.K., Wang, S.K., Doores, K.J., Huang, C.Y., Pantophlet, R., Paulson, J.C., Wong, C.H., Finn, M.G., and Burton,

D.R. (2010). Defining criteria for oligomannose immunogens for HIV using icosahedral virus capsid scaffolds. Chem. Biol. *17*, 357–370.

Blattner, C., Lee, J.H., Sliepen, K., Derking, R., Falkowska, E., de la Peña, A.T., Cupo, A., Julien, J.P., van Gils, M., Lee, P.S., et al. (2014). Structural delineation of a quaternary, cleavage-dependent epitope at the gp41-gp120 interface on intact HIV-1 Env trimers. Immunity *40*, 669–680.

Bonomelli, C., Doores, K.J., Dunlop, D.C., Thaney, V., Dwek, R.A., Burton, D.R., Crispin, M., and Scanlan, C.N. (2011). The glycan shield of HIV is predominantly oligomannose independently of production system or viral clade. PLoS ONE *6*, e23521.

Bonsignori, M., Zhou, T., Sheng, Z., Chen, L., Gao, F., Joyce, M.G., Ozorowski, G., Chuang, G.Y., Schramm, C.A., Wiehe, K., et al.; NISC Comparative Sequencing Program (2016). Maturation Pathway from Germline to Broad HIV-1 Neutralizer of a CD4-Mimic Antibody. Cell *165*, 449–463.

Bowers, P.M., Verdino, P., Wang, Z., da Silva Correia, J., Chhoa, M., Macondray, G., Do, M., Neben, T.Y., Horlick, R.A., Stanfield, R.L., et al. (2014). Nucleotide insertions and deletions complement point mutations to massively expand the diversity created by somatic hypermutation of antibodies. J. Biol. Chem. *289*, 33557–33567.

Bradley, T., Fera, D., Bhiman, J., Eslamizar, L., Lu, X., Anasti, K., Zhang, R., Sutherland, L.L., Scearce, R.M., Bowman, C.M., et al. (2016). Structural Constraints of Vaccine-Induced Tier-2 Autologous HIV Neutralizing Antibodies Targeting the Receptor-Binding Site. Cell Rep. *14*, 43–54.

Burton, D.R., Ahmed, R., Barouch, D.H., Butera, S.T., Crotty, S., Godzik, A., Kaufmann, D.E., McElrath, M.J., Nussenzweig, M.C., Pulendran, B., et al. (2012). A Blueprint for HIV Vaccine Discovery. Cell Host Microbe *12*, 396–407.

Calarese, D.A., Scanlan, C.N., Zwick, M.B., Deechongkit, S., Mimura, Y., Kunert, R., Zhu, P., Wormald, M.R., Stanfield, R.L., Roux, K.H., et al. (2003). Antibody domain exchange is an immunological solution to carbohydrate cluster recognition. Science *300*, 2065–2071.

Corti, D., and Lanzavecchia, A. (2013). Broadly neutralizing antiviral antibodies. Annu. Rev. Immunol. *31*, 705–742.

Crispin, M., Harvey, D.J., Chang, V.T., Yu, C., Aricescu, A.R., Jones, E.Y., Davis, S.J., Dwek, R.A., and Rudd, P.M. (2006). Inhibition of hybrid- and complex-type glycosylation reveals the presence of the GlcNAc transferase I-independent fucosylation pathway. Glycobiology *16*, 748–756.

Crooks, E.T., Tong, T., Chakrabarti, B., Narayan, K., Georgiev, I.S., Menis, S., Huang, X., Kulp, D., Osawa, K., Muranaka, J., et al. (2015). Vaccine-Elicited Tier 2 HIV-1 Neutralizing Antibodies Bind to Quaternary Epitopes Involving Glycan-Deficient Patches Proximal to the CD4 Binding Site. PLoS Pathog. *11*, e1004932.

de Taeye, S.W., Ozorowski, G., Torrents de la Peña, A., Guttman, M., Julien, J.P., van den Kerkhof, T.L., Burger, J.A., Pritchard, L.K., Pugach, P., Yasmeen, A., et al. (2015). Immunogenicity of Stabilized HIV-1 Envelope Trimers with Reduced Exposure of Non-neutralizing Epitopes. Cell *163*, 1702–1715.

DeLano, W.L. (2012). The PyMOL Molecular Graphics System (Schrödinger, LLC).

Deshaw, M., and Pirofski, L.A. (1995). Antibodies to the Cryptococcus neoformans capsular glucuronoxylomannan are ubiquitous in serum from HIV+ and HIV- individuals. Clin. Exp. Immunol. *99*, 425–432.

Doores, K.J. (2015). The HIV glycan shield as a target for broadly neutralizing antibodies. FEBS J. *282*, 4679–4691.

Doores, K.J., and Burton, D.R. (2010). Variable loop glycan dependency of the broad and potent HIV-1-neutralizing antibodies PG9 and PG16. J. Virol. *84*, 10510–10521.

Doores, K.J., Bonomelli, C., Harvey, D.J., Vasiljevic, S., Dwek, R.A., Burton, D.R., Crispin, M., and Scanlan, C.N. (2010a). Envelope glycans of immunodeficiency virions are almost entirely oligomannose antigens. Proc. Natl. Acad. Sci. USA *107*, 13800–13805.

Doores, K.J., Fulton, Z., Hong, V., Patel, M.K., Scanlan, C.N., Wormald, M.R., Finn, M.G., Burton, D.R., Wilson, I.A., and Davis, B.G. (2010b). A nonself sugar mimic of the HIV glycan shield shows enhanced antigenicity. Proc. Natl. Acad. Sci. USA *107*, 17107–17112.

Doores, K.J., Kong, L., Krumm, S.A., Le, K.M., Sok, D., Laserson, U., Garces, F., Poignard, P., Wilson, I.A., and Burton, D.R. (2015). Two classes of broadly neutralizing antibodies within a single lineage directed to the high-mannose patch of HIV envelope. J. Virol. *89*, 1105–1118.

Doria-Rose, N.A., Klein, R.M., Manion, M.M., O'Dell, S., Phogat, A., Chakrabarti, B., Hallahan, C.W., Migueles, S.A., Wrammert, J., Ahmed, R., et al. (2009). Frequency and phenotype of human immunodeficiency virus envelope-specific B cells from patients with broadly cross-neutralizing antibodies. J. Virol. *83*, 188–199.

Doria-Rose, N.A., Schramm, C.A., Gorman, J., Moore, P.L., Bhiman, J.N., DeKosky, B.J., Ernandes, M.J., Georgiev, I.S., Kim, H.J., Pancera, M., et al.; NISC Comparative Sequencing Program (2014). Developmental pathway for potent V1V2-directed HIV-neutralizing antibodies. Nature *509*, 55–62.

Dunlop, D.C., Bonomelli, C., Mansab, F., Vasiljevic, S., Doores, K.J., Wormald, M.R., Palma, A.S., Feizi, T., Harvey, D.J., Dwek, R.A., et al. (2010). Polysaccharide mimicry of the epitope of the broadly neutralizing anti-HIV antibody, 2G12, induces enhanced antibody responses to self oligomannose glycans. Glycobiology *20*, 812–823.

Eggink, D., Melchers, M., Wuhrer, M., van Montfort, T., Dey, A.K., Naaijkens, B.A., David, K.B., Le Douce, V., Deelder, A.M., Kang, K., et al. (2010). Lack of complex N-glycans on HIV-1 envelope glycoproteins preserves protein conformation and entry function. Virology *401*, 236–247.

Escolano, A., Steichen, J.M., Dosenovic, P., Kulp, D.W., Golijanin, J., Sok, D., Freund, N.T., Gitlin, A.D., Oliveira, T., Araki, T., et al. (2016). Sequential immunization elicits broadly neutralizing anti-HIV-1 antibodies in Ig knockin mice. Cell *166*, 1445–1458.

Fauci, A.S., and Marston, H.D. (2014). Ending AIDS–is an HIV vaccine necessary? N. Engl. J. Med. *370*, 495–498.

Garces, F., Sok, D., Kong, L., McBride, R., Kim, H.J., Saye-Francisco, K.F., Julien, J.P., Hua, Y., Cupo, A., Moore, J.P., et al. (2014). Structural evolution of glycan recognition by a family of potent HIV antibodies. Cell *159*, 69–79.

Garces, F., Lee, J.H., de Val, N., de la Pena, A.T., Kong, L., Puchades, C., Hua, Y., Stanfield, R.L., Burton, D.R., Moore, J.P., et al. (2015). Affinity Maturation of a Potent Family of HIV Antibodies Is Primarily Focused on Accommodating or Avoiding Glycans. Immunity *43*, 1053–1063.

Go, E.P., Irungu, J., Zhang, Y., Dalpathado, D.S., Liao, H.X., Sutherland, L.L., Alam, S.M., Haynes, B.F., and Desaire, H. (2008). Glycosylation site-specific analysis of HIV envelope proteins (JR-FL and CON-S) reveals major differences in glycosylation site occupancy, glycoform profiles, and antigenic epitopes' accessibility. J. Proteome Res. *7*, 1660–1674.

Go, E.P., Liao, H.X., Alam, S.M., Hua, D., Haynes, B.F., and Desaire, H. (2013). Characterization of host-cell line specific glycosylation profiles of early transmitted/founder HIV-1 gp120 envelope proteins. J. Proteome Res. *12*, 1223–1234.

Go, E.P., Herschhorn, A., Gu, C., Castillo-Menendez, L., Zhang, S., Mao, Y., Chen, H., Ding, H., Wakefield, J.K., Hua, D., et al. (2015). Comparative Analysis of the Glycosylation Profiles of Membrane-Anchored HIV-1 Envelope Glycoprotein Trimers and Soluble gp140. J. Virol. *89*, 8245–8257.

Gray, E.S., Madiga, M.C., Hermanus, T., Moore, P.L., Wibmer, C.K., Tumba, N.L., Werner, L., Mlisana, K., Sibeko, S., Williamson, C., et al.; CAPRISA002 Study Team (2011). The neutralization breadth of HIV-1 develops incrementally over four years and is associated with CD4+ T cell decline and high viral load during acute infection. J. Virol. *85*, 4828–4840.

Hangartner, L., Zinkernagel, R.M., and Hengartner, H. (2006). Antiviral antibody responses: the two extremes of a wide spectrum. Nat. Rev. Immunol. *6*, 231–243.

Haynes, B.F., and Verkoczy, L. (2014). AIDS/HIV. Host controls of HIV neutralizing antibodies. Science *344*, 588–589.

Haynes, B.F., Kelsoe, G., Harrison, S.C., and Kepler, T.B. (2012). B-cell-lineage immunogen design in vaccine development with HIV-1 as a case study. Nat. Biotechnol. *30*, 423–433.

Im, W., Beglov, D., and Roux, B. (1998). Continuum solvation model: computation of electrostatic forces from numerical solutions to the Poisson-Boltzmann equation. Comput. Phys. Commun. *111*, 59–75.

Jo, S., Kim, T., Iyer, V.G., and Im, W. (2008a). CHARMM-GUI: a web-based graphical user interface for CHARMM. J. Comput. Chem. *29*, 1859–1865.

Jo, S., Vargyas, M., Vasko-Szedlar, J., Roux, B., and Im, W. (2008b). PBEQ-Solver for online visualization of electrostatic potential of biomolecules. Nucleic Acids Res. *36*, W270–W275.

Joyce, J.G., Krauss, I.J., Song, H.C., Opalka, D.W., Grimm, K.M., Nahas, D.D., Esser, M.T., Hrin, R., Feng, M., Dudkin, V.Y., et al. (2008). An oligosaccharide-based HIV-1 2G12 mimotope vaccine induces carbohydrate-specific antibodies that fail to neutralize HIV-1 virions. Proc. Natl. Acad. Sci. USA *105*, 15684–15689.

Julien, J.P., Cupo, A., Sok, D., Stanfield, R.L., Lyumkis, D., Deller, M.C., Klasse, P.J., Burton, D.R., Sanders, R.W., Moore, J.P., et al. (2013). Crystal structure of a soluble cleaved HIV-1 envelope trimer. Science *342*, 1477–1483.

Kepler, T.B. (2013). Reconstructing a B-cell clonal lineage. I. Statistical inference of unobserved ancestors. F1000Res. *2*, 103.

Kepler, T.B., Liao, H.X., Alam, S.M., Bhaskarabhatla, R., Zhang, R., Yandava, C., Stewart, S., Anasti, K., Kelsoe, G., Parks, R., et al. (2014). Immunoglobulin gene insertions and deletions in the affinity maturation of HIV-1 broadly reactive neutralizing antibodies. Cell Host Microbe *16*, 304–313.

Kong, L., Lee, J.H., Doores, K.J., Murin, C.D., Julien, J.P., McBride, R., Liu, Y., Marozsan, A., Cupo, A., Klasse, P.J., et al. (2013). Supersite of immune vulnerability on the glycosylated face of HIV-1 envelope glycoprotein gp120. Nat. Struct. Mol. Biol. *20*, 796–803.

Kuraoka, M., Schmidt, A.G., Nojima, T., Feng, F., Watanabe, A., Kitamura, D., Harrison, S.C., Kepler, T.B., and Kelsoe, G. (2016). Complex Antigens Drive Permissive Clonal Selection in Germinal Centers. Immunity *44*, 542–552.

Leonard, C.K., Spellman, M.W., Riddle, L., Harris, R.J., Thomas, J.N., and Gregory, T.J. (1990). Assignment of intrachain disulfide bonds and characterization of potential glycosylation sites of the type 1 recombinant human immunodeficiency virus envelope glycoprotein (gp120) expressed in Chinese hamster ovary cells. J. Biol. Chem. *265*, 10373–10382.

Liao, H.X., Levesque, M.C., Nagel, A., Dixon, A., Zhang, R., Walter, E., Parks, R., Whitesides, J., Marshall, D.J., Hwang, K.K., et al. (2009). High-throughput isolation of immunoglobulin genes from single human B cells and expression as monoclonal antibodies. J. Virol. Methods *158*, 171–179.

Liao, H.X., Lynch, R., Zhou, T., Gao, F., Alam, S.M., Boyd, S.D., Fire, A.Z., Roskin, K.M., Schramm, C.A., Zhang, Z., et al.; NISC Comparative Sequencing Program (2013a). Co-evolution of a broadly neutralizing HIV-1 antibody and founder virus. Nature *496*, 469–476.

Liao, H.X., Tsao, C.Y., Alam, S.M., Muldoon, M., Vandergrift, N., Ma, B.J., Lu, X., Sutherland, L.L., Scearce, R.M., Bowman, C., et al. (2013b). Antigenicity and immunogenicity of transmitted/founder, consensus, and chronic envelope glycoproteins of human immunodeficiency virus type 1. J. Virol. *87*, 4185–4201.

MacLeod, D.T., Choi, N.M., Briney, B., Garces, F., Ver, L.S., Landais, E., Murrell, B., Wrin, T., Kilembe, W., Liang, C.H., et al.; IAVI Protocol C Investigators & The IAVI African HIV Research Network (2016). Early Antibody Lineage Diversification and Independent Limb Maturation Lead to Broad HIV-1 Neutralization Targeting the Env High-Mannose Patch. Immunity *44*, 1215–1226.

Mascola, J.R., and Haynes, B.F. (2013). HIV-1 neutralizing antibodies: understanding nature's pathways. Immunol. Rev. *254*, 225–244.

Mascola, J.R., and Montefiori, D.C. (2010). The role of antibodies in HIV vaccines. Annu. Rev. Immunol. *28*, 413–444.

McCoy, L.E., van Gils, M.J., Ozorowski, G., Messmer, T., Briney, B., Voss, J.E., Kulp, D.W., Macauley, M.S., Sok, D., Pauthner, M., et al. (2016). Holes in the Glycan Shield of the Native HIV Envelope Are a Target of Trimer-Elicited Neutralizing Antibodies. Cell Rep. *16*, 2327–2338.

McLellan, J.S., Pancera, M., Carrico, C., Gorman, J., Julien, J.P., Khayat, R., Louder, R., Pejchal, R., Sastry, M., Dai, K., et al. (2011). Structure of HIV-1 gp120 V1/V2 domain with broadly neutralizing antibody PG9. Nature *480*, 336–343.

Moldt, B., Rakasz, E.G., Schultz, N., Chan-Hui, P.Y., Swiderek, K., Weisgrau, K.L., Piaskowski, S.M., Bergman, Z., Watkins, D.I., Poignard, P., and Burton, D.R. (2012). Highly potent HIV-specific antibody neutralization in vitro translates into effective protection against mucosal SHIV challenge in vivo. Proc. Natl. Acad. Sci. USA *109*, 18921–18925.

Moody, M.A., Yates, N.L., Amos, J.D., Drinker, M.S., Eudailey, J.A., Gurley, T.C., Marshall, D.J., Whitesides, J.F., Chen, X., Foulger, A., et al. (2012). HIV-1 gp120 vaccine induces affinity maturation in both new and persistent antibody clonal lineages. J. Virol. *86*, 7496–7507.

Murin, C.D., Julien, J.P., Sok, D., Stanfield, R.L., Khayat, R., Cupo, A., Moore, J.P., Burton, D.R., Wilson, I.A., and Ward, A.B. (2014). Structure of 2G12 Fab2 in complex with soluble and fully glycosylated HIV-1 Env by negative-stain single-particle electron microscopy. J. Virol. *88*, 10177–10188.

Pancera, M., Zhou, T., Druz, A., Georgiev, I.S., Soto, C., Gorman, J., Huang, J., Acharya, P., Chuang, G.Y., Ofek, G., et al. (2014). Structure and immune recognition of trimeric pre-fusion HIV-1 Env. Nature *514*, 455–461.

Parren, P.W., and Burton, D.R. (2001). The antiviral activity of antibodies in vitro and in vivo. Adv. Immunol. *77*, 195–262.

Pejchal, R., Doores, K.J., Walker, L.M., Khayat, R., Huang, P.S., Wang, S.K., Stanfield, R.L., Julien, J.P., Ramos, A., Crispin, M., et al. (2011). A potent and broad neutralizing antibody recognizes and penetrates the HIV glycan shield. Science *334*, 1097–1103.

Reeves, P.J., Callewaert, N., Contreras, R., and Khorana, H.G. (2002). Structure and function in rhodopsin: high-level expression of rhodopsin with restricted and homogeneous N-glycosylation by a tetracycline-inducible N-acetylglucosaminyltransferase I-negative HEK293S stable mammalian cell line. Proc. Natl. Acad. Sci. USA *99*, 13419–13424.

Sanders, R.W., van Gils, M.J., Derking, R., Sok, D., Ketas, T.J., Burger, J.A., Ozorowski, G., Cupo, A., Simonich, C., Goo, L., et al. (2015). HIV-1 VACCINES. HIV-1 neutralizing antibodies induced by native-like envelope trimers. Science *349*, aac4223.

Sather, D.N., Armann, J., Ching, L.K., Mavrantoni, A., Sellhorn, G., Caldwell, Z., Yu, X., Wood, B., Self, S., Kalams, S., and Stamatatos, L. (2009). Factors associated with the development of cross-reactive neutralizing antibodies during human immunodeficiency virus type 1 infection. J. Virol. *83*, 757–769.

Scanlan, C.N., Offer, J., Zitzmann, N., and Dwek, R.A. (2007a). Exploiting the defensive sugars of HIV-1 for drug and vaccine design. Nature *446*, 1038–1045.

Scanlan, C.N., Ritchie, G.E., Baruah, K., Crispin, M., Harvey, D.J., Singer, B.B., Lucka, L., Wormald, M.R., Wentworth, P., Jr., Zitzmann, N., et al. (2007b). Inhibition of mammalian glycan biosynthesis produces non-self antigens for a broadly neutralising, HIV-1 specific antibody. J. Mol. Biol. *372*, 16–22.

Simek, M.D., Rida, W., Priddy, F.H., Pung, P., Carrow, E., Laufer, D.S., Lehrman, J.K., Boaz, M., Tarragona-Fiol, T., Miiro, G., et al. (2009). Human immunodeficiency virus type 1 elite neutralizers: individuals with broad and potent neutralizing activity identified by using a high-throughput neutralization assay together with an analytical selection algorithm. J. Virol. *83*, 7337–7348.

Simonich, C.A., Williams, K.L., Verkerke, H.P., Williams, J.A., Nduati, R., Lee, K.K., and Overbaugh, J. (2016). HIV-1 Neutralizing Antibodies with Limited Hypermutation from an Infant. Cell *166*, 77–87.

Sok, D., Pauthner, M., Briney, B., Lee, J.H., Saye-Francisco, K.L., Hsueh, J., Ramos, A., Le, K.M., Jones, M., Jardine, J.G., et al. (2016). A Prominent Site of Antibody Vulnerability on HIV Envelope Incorporates a Motif Associated with CCR5 Binding and Its Camouflaging Glycans. Immunity *45*, 31–45.

Steichen, J.M., Kulp, D.W., Tokatlian, T., Escolano, A., Dosenovic, P., Stanfield, R.L., McCoy, L.E., Ozorowski, G., Hu, X., Kalyuzhniy, O., et al. (2016). HIV Vaccine Design to Target Germline Precursors of Glycan-Dependent Broadly Neutralizing Antibodies. Immunity *45*, 483–496.

Tian, M., Cheng, C., Chen, X., Duan, H., Cheng, H.L., Dao, M., Sheng, Z., Kimble, M., Wang, L., Lin, S., et al. (2016). Induction of HIV Neutralizing Antibody Lineages in Mice with Diverse Precursor Repertoires. Cell *166*, 1471–1484.

Volpe, J.M., Cowell, L.G., and Kepler, T.B. (2006). SoDA: implementation of a 3D alignment algorithm for inference of antigen receptor recombinations. Bioinformatics 22, 438–444.

Walker, L.M., Phogat, S.K., Chan-Hui, P.Y., Wagner, D., Phung, P., Goss, J.L., Wrin, T., Simek, M.D., Fling, S., Mitcham, J.L., et al.; Protocol G Principal Investigators (2009). Broad and potent neutralizing antibodies from an African donor reveal a new HIV-1 vaccine target. Science 326, 285–289.

Walker, L.M., Simek, M.D., Priddy, F., Gach, J.S., Wagner, D., Zwick, M.B., Phogat, S.K., Poignard, P., and Burton, D.R. (2010). A limited number of antibody specificities mediate broad and potent serum neutralization in selected HIV-1 infected individuals. PLoS Pathog. 6, e1001028.

Walker, L.M., Huber, M., Doores, K.J., Falkowska, E., Pejchal, R., Julien, J.P., Wang, S.K., Ramos, A., Chan-Hui, P.Y., Moyle, M., et al.; Protocol G Principal Investigators (2011). Broad neutralization coverage of HIV by multiple highly potent antibodies. Nature 477, 466–470.

Wang, S.K., Liang, P.H., Astronomo, R.D., Hsu, T.L., Hsieh, S.L., Burton, D.R., and Wong, C.H. (2008). Targeting the carbohydrates on HIV-1: Interaction of oligomannose dendrons with human monoclonal antibody 2G12 and DC-SIGN. Proc. Natl. Acad. Sci. USA 105, 3690–3695.

Wei, X., Decker, J.M., Wang, S., Hui, H., Kappes, J.C., Wu, X., Salazar-Gonzalez, J.F., Salazar, M.G., Kilby, J.M., Saag, M.S., et al. (2003). Antibody neutralization and escape by HIV-1. Nature 422, 307–312.

Wiehe, K., Easterhoff, D., Luo, K., Nicely, N.I., Bradley, T., Jaeger, F.H., Dennison, S.M., Zhang, R., Lloyd, K.E., Stolarchuk, C., et al. (2014). Antibody light-chain-restricted recognition of the site of immune pressure in the RV144 HIV-1 vaccine trial is phylogenetically conserved. Immunity 41, 909–918.

Zhang, H., Fu, H., Luallen, R.J., Liu, B., Lee, F.H., Doms, R.W., and Geng, Y. (2015). Antibodies elicited by yeast glycoproteins recognize HIV-1 virions and potently neutralize virions with high mannose N-glycans. Vaccine 33, 5140–5147.

Zhang, R., Verkoczy, L., Wiehe, K., Munir Alam, S., Nicely, N.I., Santra, S., Bradley, T., Pemble, C.W., 4th, Zhang, J., Gao, F., et al. (2016). Initiation of immune tolerance-controlled HIV gp41 neutralizing B cell lineages. Sci. Transl. Med. 8, 336ra62.

Zhou, T., Zhu, J., Wu, X., Moquin, S., Zhang, B., Acharya, P., Georgiev, I.S., Altae-Tran, H.R., Chuang, G.Y., Joyce, M.G., et al.; NISC Comparative Sequencing Program (2013). Multidonor analysis reveals structural elements, genetic determinants, and maturation pathway for HIV-1 neutralization by VRC01-class antibodies. Immunity 39, 245–258.